DESY 95-36 ISSN 0418-9833
February 1995

# First Measurement of the Deep–Inelastic Structure of Proton Diffraction

H1 Collaboration

**Abstract**

A measurement is presented, using data taken with the H1 detector at HERA, of the contribution of diffractive interactions to deep–inelastic electron–proton ($ep$) scattering in the kinematic range $8.5 < Q^2 < 50\,\mathrm{GeV}^2$, $2.4 \times 10^{-4} <$ Bjorken–$x < 0.0133$, and $3.7 \times 10^{-4} < x_{I\!P} < 0.043$. The diffractive contribution to the proton structure function $F_2(x, Q^2)$ is evaluated as a function of the appropriate deep–inelastic scattering variables $x_{I\!P}$, $Q^2$, and $\beta$ $(= x/x_{I\!P})$ using a class of deep–inelastic $ep$ scattering events with no hadronic energy flow in an interval of pseudo–rapidity adjacent to the proton beam direction. The dependence of this contribution on $x_{I\!P}$ is measured to be $x_{I\!P}^{-n}$ with $n = 1.19 \pm 0.06(stat.) \pm 0.07(syst.)$ independent of $\beta$ and $Q^2$, which is consistent with both a diffractive interpretation and a factorisable $ep$ diffractive cross section. A first measurement of the deep–inelastic structure of the pomeron in the form of the $Q^2$ and $\beta$ dependences of a factorised structure function is presented. For all measured $\beta$, this structure function is observed to be consistent with scale invariance.

*Submitted to Physics Letters* ***B***

T. Ahmed[3], S. Aid[13], V. Andreev[24], B. Andrieu[28], R.-D. Appuhn[11], M. Arpagaus[36], A. Babaev[26], J. Baehr[35], J. Bán[17], Y. Ban[27], P. Baranov[24], E. Barrelet[29], W. Bartel[11], M. Barth[4], U. Bassler[29], H.P. Beck[37], H.-J. Behrend[11], A. Belousov[24], Ch. Berger[1], G. Bernardi[29], R. Bernet[36], G. Bertrand-Coremans[4], M. Besançon[9], R. Beyer[11], P. Biddulph[22], P. Bispham[22], J.C. Bizot[27], V. Blobel[13], K. Borras[8], F. Botterweck[4], V. Boudry[7], A. Braemer[14], F. Brasse[11], W. Braunschweig[1], V. Brisson[27], D. Bruncko[17], C. Brune[15], R.Buchholz[11], L. Büngener[13], J. Bürger[11], F.W. Büsser[13], A. Buniatian[11,39], S. Burke[18], M. Burton[22], G. Buschhorn[26], A.J. Campbell[11], T. Carli[26], F. Charles[11], D. Clarke[5], A.B. Clegg[18], B. Clerbaux[4], M. Colombo[8], J.G. Contreras[8], C. Cormack[19], J.A. Coughlan[5], A. Courau[27], Ch. Coutures[9], G. Cozzika[9], L. Criegee[11], D.G. Cussans[5], J. Cvach[30], S. Dagoret[29], J.B. Dainton[19], W.D. Dau[16], K. Daum[34], M. David[9], E. Deffur[11], B. Delcourt[27], L. Del Buono[29], A. De Roeck[11], E.A. De Wolf[4], P. Di Nezza[32], C. Dollfus[37], J.D. Dowell[3], H.B. Dreis[2], A. Droutskoi[23], J. Duboc[29], D. Düllmann[13], O. Dünger[13], H. Duhm[12], J. Ebert[34], T.R. Ebert[19], G. Eckerlin[11], V. Efremenko[23], S. Egli[37], H. Ehrlichmann[35], S. Eichenberger[37], R. Eichler[36], F. Eisele[14], E. Eisenhandler[20], R.J. Ellison[22], E. Elsen[11], M. Erdmann[14], W. Erdmann[36], E. Evrard[4], L. Favart[4], A. Fedotov[23], D. Feeken[13], R. Felst[11], J. Feltesse[9], J. Ferencei[15], F. Ferrarotto[32], K. Flamm[11], M. Fleischer[11], M. Flieser[26], G. Flügge[2], A. Fomenko[24], M. Forbush[7], J. Formánek[31], J.M. Foster[22], G. Franke[11], E. Fretwurst[12], E. Gabathuler[19], K. Gabathuler[33], K. Gamerdinger[26], J. Garvey[3], J. Gayler[11], M. Gebauer[8], A. Gellrich[11], H. Genzel[1], R. Gerhards[11], U. Goerlach[11], L. Goerlich[6], N. Gogitidze[24], M. Goldberg[29], D. Goldner[8], B. Gonzalez-Pineiro[29], I. Gorelov[23], P. Goritchev[23], C. Grab[36], H. Grässler[2], R. Grässler[2], T. Greenshaw[19], G. Grindhammer[26], A. Gruber[26], C. Gruber[16], J. Haack[35], D. Haidt[11], L. Hajduk[6], O. Hamon[29], M. Hampel[1], E.M. Hanlon[18], M. Hapke[11], W.J. Haynes[5], J. Heatherington[20], G. Heinzelmann[13], R.C.W. Henderson[18], H. Henschel[35], I. Herynek[30], M.F. Hess[26], W. Hildesheim[11], P. Hill[5], K.H. Hiller[35], C.D. Hilton[22], J. Hladký[30], K.C. Hoeger[22], M. Höppner[8], R. Horisberger[33], V.L. Hudgson[3], Ph. Huet[4], M. Hütte[8], H. Hufnagel[14], M. Ibbotson[22], H. Itterbeck[1], M.-A. Jabiol[9], A. Jacholkowska[27], C. Jacobsson[21], M. Jaffre[27], J. Janoth[15], T. Jansen[11], L. Jönsson[21], D.P. Johnson[4], L. Johnson[18], H. Jung[29], P.I.P. Kalmus[20], D. Kant[20], R. Kaschowitz[2], P. Kasselmann[12], U. Kathage[16], J. Katzy[14], H.H. Kaufmann[35], S. Kazarian[11], I.R. Kenyon[3], S. Kermiche[25], C. Keuker[1], C. Kiesling[26], M. Klein[35], C. Kleinwort[13], G. Knies[11], W. Ko[7], T. Köhler[1], J.H. Köhne[26], H. Kolanoski[8], F. Kole[7], S.D. Kolya[22], V. Korbel[11], M. Korn[8], P. Kostka[35], S.K. Kotelnikov[24], T. Krämerkämper[8], M.W. Krasny[6,29], H. Krehbiel[11], D. Krücker[2], U. Krüger[11], U. Krüner-Marquis[11], J.P. Kubenka[26], H. Küster[2], M. Kuhlen[26], T. Kurča[17], J. Kurzhöfer[8], B. Kuznik[34], D. Lacour[29], F. Lamarche[28], R. Lander[7], M.P.J. Landon[20], W. Lange[35], P. Lanius[26], J.-F. Laporte[9], A. Lebedev[24], C. Leverenz[11], S. Levonian[24], Ch. Ley[2], A. Lindner[8], G. Lindström[12], J. Link[7], F. Linsel[11], J. Lipinski[13], B. List[11], G. Lobo[27], P. Loch[27], H. Lohmander[21], J. Lomas[22], G.C. Lopez[20], V. Lubimov[23], D. Lüke[8,11], N. Magnussen[34], E. Malinovski[24], S. Mani[7], R. Maraček[17], P. Marage[4], J. Marks[25], R. Marshall[22], J. Martens[34], R. Martin[11], H.-U. Martyn[1], J. Martyniak[6], S. Masson[2], T. Mavroidis[20], S.J. Maxfield[19], S.J. McMahon[19], A. Mehta[22], K. Meier[15], D. Mercer[22], T. Merz[11], C.A. Meyer[37], H. Meyer[34], J. Meyer[11], S. Mikocki[6], D. Milstead[19], F. Moreau[28], J.V. Morris[5], E. Mroczko[6], G. Müller[11], K. Müller[37], P. Murín[17], V. Nagovizin[23], R. Nahnhauer[35], B. Naroska[13], Th. Naumann[35], P.R. Newman[3], D. Newton[18], D. Neyret[29], H.K. Nguyen[29], T.C. Nicholls[3], F. Niebergall[13], C. Niebuhr[11], Ch. Niedzballa[1], R. Nisius[1], G. Nowak[6], G.W. Noyes[5], M. Nyberg-Werther[21], M. Oakden[19], H. Oberlack[26], U. Obrock[8], J.E. Olsson[11], D. Ozerov[23], E. Panaro[11], A. Panitch[4], C. Pascaud[27], G.D. Patel[19], E. Peppel[35], E. Perez[9], J.P. Phillips[22], Ch. Pichler[12], D. Pitzl[36], G. Pope[7], S. Prell[11], R. Prosi[11], K. Rabbertz[1], G. Rädel[11], F. Raupach[1], P. Reimer[30], S. Reinshagen[11], P. Ribarics[26], H.Rick[8], V. Riech[12], J. Riedlberger[36], S. Riess[13], M. Rietz[2], E. Rizvi[20], S.M. Robertson[3], P. Robmann[37], H.E. Roloff[35], R. Roosen[4], K. Rosenbauer[1] A. Rostovtsev[23], F. Rouse[7], C. Royon[9], K. Rüter[26], S. Rusakov[24], K. Rybicki[6], R. Rylko[20], N. Sahlmann[2], E. Sanchez[26], D.P.C. Sankey[5], P. Schacht[26], S. Schiek[11], P. Schleper[14],

W. von Schlippe[20], C. Schmidt[11], D. Schmidt[34], G. Schmidt[13], A. Schöning[11], V. Schröder[11], E. Schuhmann[26], B. Schwab[14], A. Schwind[35], F. Sefkow[11], M. Seidel[12], R. Sell[11], A. Semenov[23], V. Shekelyan[11], I. Sheviakov[24], H. Shooshtari[26], L.N. Shtarkov[24], G. Siegmon[16], U. Siewert[16], Y. Sirois[28], I.O. Skillicorn[10], P. Smirnov[24], J.R. Smith[7], V. Solochenko[23], Y. Soloviev[24], J. Spiekermann[8], H. Spitzer[13], R. Starosta[1], M. Steenbock[13], P. Steffen[11], R. Steinberg[2], B. Stella[32], K. Stephens[22], J. Stier[11], J. Stiewe[15], U. Stösslein[35], K. Stolze[35], J. Strachota[30], U. Straumann[37], W. Struczinski[2], J.P. Sutton[3], S. Tapprogge[15], R.E. Taylor[38,27], V. Tchernyshov[23], C. Thiebaux[28], G. Thompson[20], P. Truöl[37], J. Turnau[6], J. Tutas[14], P. Uelkes[2], A. Usik[24], S. Valkár[31], A. Valkárová[31], C. Vallée[25], P. Van Esch[4], P. Van Mechelen[4], A. Vartapetian[11,39], Y. Vazdik[24], P. Verrecchia[9], G. Villet[9], K. Wacker[8], A. Wagener[2], M. Wagener[33], I.W. Walker[18], A. Walther[8], G. Weber[13], M. Weber[11], D. Wegener[8], A. Wegner[11], H.P. Wellisch[26], L.R. West[3], S. Willard[7], M. Winde[35], G.-G. Winter[11], C. Wittek[13], A.E. Wright[22], E. Wünsch[11], N. Wulff[11], T.P. Yiou[29], J. Žáček[31], D. Zarbock[12], Z. Zhang[27], A. Zhokin[23], M. Zimmer[11], W. Zimmermann[11], F. Zomer[27], and K. Zuber[15]

[1] I. Physikalisches Institut der RWTH, Aachen, Germany[a]
[2] III. Physikalisches Institut der RWTH, Aachen, Germany[a]
[3] School of Physics and Space Research, University of Birmingham, Birmingham, UK[b]
[4] Inter-University Institute for High Energies ULB-VUB, Brussels; Universitaire Instelling Antwerpen, Wilrijk, Belgium[c]
[5] Rutherford Appleton Laboratory, Chilton, Didcot, UK[b]
[6] Institute for Nuclear Physics, Cracow, Poland[d]
[7] Physics Department and IIRPA, University of California, Davis, California, USA[e]
[8] Institut für Physik, Universität Dortmund, Dortmund, Germany[a]
[9] CEA, DSM/DAPNIA, CE-Saclay, Gif-sur-Yvette, France
[10] Department of Physics and Astronomy, University of Glasgow, Glasgow, UK[b]
[11] DESY, Hamburg, Germany[a]
[12] I. Institut für Experimentalphysik, Universität Hamburg, Hamburg, Germany[a]
[13] II. Institut für Experimentalphysik, Universität Hamburg, Hamburg, Germany[a]
[14] Physikalisches Institut, Universität Heidelberg, Heidelberg, Germany[a]
[15] Institut für Hochenergiephysik, Universität Heidelberg, Heidelberg, Germany[a]
[16] Institut für Reine und Angewandte Kernphysik, Universität Kiel, Kiel, Germany[a]
[17] Institute of Experimental Physics, Slovak Academy of Sciences, Košice, Slovak Republic[f]
[18] School of Physics and Materials, University of Lancaster, Lancaster, UK[b]
[19] Department of Physics, University of Liverpool, Liverpool, UK[b]
[20] Queen Mary and Westfield College, London, UK[b]
[21] Physics Department, University of Lund, Lund, Sweden[g]
[22] Physics Department, University of Manchester, Manchester, UK[b]
[23] Institute for Theoretical and Experimental Physics, Moscow, Russia
[24] Lebedev Physical Institute, Moscow, Russia[f]
[25] CPPM, Université d'Aix-Marseille II, IN2P3-CNRS, Marseille, France
[26] Max-Planck-Institut für Physik, München, Germany[a]
[27] LAL, Université de Paris-Sud, IN2P3-CNRS, Orsay, France
[28] LPNHE, Ecole Polytechnique, IN2P3-CNRS, Palaiseau, France
[29] LPNHE, Universités Paris VI and VII, IN2P3-CNRS, Paris, France
[30] Institute of Physics, Czech Academy of Sciences, Praha, Czech Republic[f,h]
[31] Nuclear Center, Charles University, Praha, Czech Republic[f,h]
[32] INFN Roma and Dipartimento di Fisica, Universita "La Sapienza", Roma, Italy
[33] Paul Scherrer Institut, Villigen, Switzerland
[34] Fachbereich Physik, Bergische Universität Gesamthochschule Wuppertal, Wuppertal, Germany[a]
[35] DESY, Institut für Hochenergiephysik, Zeuthen, Germany[a]

[36] Institut für Teilchenphysik, ETH, Zürich, Switzerland[i]
[37] Physik-Institut der Universität Zürich, Zürich, Switzerland[i]
[38] Stanford Linear Accelerator Center, Stanford California, USA
[39] Visitor from Yerevan Phys.Inst., Armenia

[a] Supported by the Bundesministerium für Forschung und Technologie, FRG under contract numbers 6AC17P, 6AC47P, 6DO57I, 6HH17P, 6HH27I, 6HD17I, 6HD27I, 6KI17P, 6MP17I, and 6WT87P
[b] Supported by the UK Particle Physics and Astronomy Research Council, and formerly by the UK Science and Engineering Research Council
[c] Supported by FNRS-NFWO, IISN-IIKW
[d] Supported by the Polish State Committee for Scientific Research, grant No. 204209101
[e] Supported in part by USDOE grant DE F603 91ER40674
[f] Supported by the Deutsche Forschungsgemeinschaft
[g] Supported by the Swedish Natural Science Research Council
[h] Supported by GA ČR, grant no. 202/93/2423 and by GA AV ČR, grant no. 19095
[i] Supported by the Swiss National Science Foundation

## 1 Introduction and Formalism

Recent measurements at HERA of deep–inelastic electron–proton ($ep$) scattering (DIS) in the low Bjorken–$x$ kinematic range $5 < Q^2 < 120\,\mathrm{GeV}^2$ and $10^{-4} < x < 10^{-2}$ have demonstrated the existence of a distinct class of events in which there is no hadronic energy flow in an interval of (laboratory frame) pseudo–rapidity $\eta$ adjacent to the proton beam direction [1, 2]. Our present understanding of DIS could be inadequate at low $x$ because additions to the leading order QCD–based partonic picture are likely to be substantial. A natural interpretation of these so called "rapidity gap" events is based on the hypothesis that the deep–inelastic scattering process involves the interaction of the virtual boson probe with a colourless component of the proton. Hence there is no chromodynamic radiation in the final state immediately adjacent to the direction of the scattered proton or any proton remnant. Observed distributions of such events are found to be consistent with simulations based on models in which the virtual boson–proton interaction is diffractive [2], that is in which the colourless component of the proton is hypothesised to be a pomeron ($I\!P$) and the virtual boson–proton interaction may be understood as $I\!P$ exchange. The observation of these rapidity gap events in DIS means that a measurement of any short distance sub–structure of this colourless component of the proton is possible, and thus, if the process is diffractive, of the $I\!P$. An understanding of the sub–structure of this colourless component, whether in the form of a partonic interpretation [3, 4, 5] or otherwise, is essential for further understanding of the partonic picture of deep–inelastic lepton–nucleon scattering.

In this paper we present a measurement which quantifies the contribution of rapidity gap events to the inclusive deep–inelastic structure function $F_2$ of the proton. The results here follow our first measurement of this contribution in terms of a "diffractive structure function" $F_2^D$ as a function of the two DIS variables $x$ and $Q^2$ reported in [6]. The measurement presented here is made as a function of the three kinematic variables $\beta$, $Q^2$, and $x$, or equivalently $\beta$, $Q^2$, and $x_{I\!P}$, which are defined as follows:

$$x = \frac{-q^2}{2P\cdot q} \qquad x_{I\!P} = \frac{q\cdot(P-P')}{q\cdot P} \qquad Q^2 = -q^2 \qquad \beta = \frac{-q^2}{2q\cdot(P-P')}. \quad (1)$$

Here $q$, $P$ and $P'$ are the 4–momenta of the virtual boson, the incident proton, and the final state colourless remnant respectively. The latter can be either a nucleon or higher mass baryonic excitation, and, if the proton interaction is diffractive, it must be a proton or a proton excitation with isospin $(I, I_3) = (\frac{1}{2}, +\frac{1}{2})$. Note that

$$x = \beta x_{I\!P}. \tag{2}$$

It is convenient to write $x_{I\!P}$ and $\beta$ above as

$$x_{I\!P} = \frac{Q^2 + M_X^2 - t}{Q^2 + W^2 - M_p^2} \approx \frac{Q^2 + M_X^2}{Q^2} \cdot x = x_{I\!P/p} \tag{3}$$

$$\beta = \frac{Q^2}{Q^2 + M_X^2 - t} \approx \frac{Q^2}{Q^2 + M_X^2} = x_{q/I\!P} \tag{4}$$

where $M_X$ is the invariant mass of the hadronic system excluding the colourless remnant, $t = (P - P')^2$ is the 4–momentum transfer squared at the incident proton vertex, and $W$ is the total hadronic invariant mass. In the kinematic domain of these measurements ($M_p^2 \ll Q^2$, $M_p^2 \ll W^2$) and if $|\,t\,|$ is small ($|\,t\,| \ll Q^2$, $|\,t\,| \ll M_X^2$) approximating to "the proton's infinite momentum frame", $x_{I\!P}$ may be interpreted as the fraction $x_{I\!P/p}$ of the 4–momentum of the proton carried by the interacting $I\!P$ (or meson for non–diffractive contributions), and $\beta$ as the fraction $x_{q/I\!P}$ of the 4–momenta of the $I\!P$ (or meson) carried by the quark interacting with the virtual boson.

The diffractive structure function $F_2^{D(3)}$, which is a function of three kinematic variables, is derived from a structure function $F_2^{D(4)}$ which is a function of the four kinematic variables $x$, $Q^2$, $x_{I\!P}$ and $t$. $F_2^{D(4)}$ is defined by analogy with the decomposition of the unpolarised total $ep$ cross section. In the $Q^2$ range of these measurements, the cross section for the process $ep \rightarrow eXp$, where here the final state $p$ specifies both nucleon and higher mass baryon excitation, is assumed to be dominated by virtual photon exchange. It is therefore written in terms of two structure functions $F_2^{D(4)}$ and $\frac{F_2^{D(4)}}{2x(1+R^{D(4)})}$ in the form ($\alpha$ is here the fine structure constant)

$$\frac{\mathrm{d}^4\sigma_{ep\rightarrow epX}}{\mathrm{d}x\mathrm{d}Q^2\mathrm{d}x_{I\!P}dt} = \frac{4\pi\alpha^2}{xQ^4}\left\{1 - y + \frac{y^2}{2[1 + R^{D(4)}(x, Q^2, x_{I\!P}, t)]}\right\} F_2^{D(4)}(x, Q^2, x_{I\!P}, t) \tag{5}$$

in which $y$ is the usual DIS scaling variable given by $y = Q^2/sx$. $s$ is the $ep$ collision centre of mass (CM) energy squared. It is convenient to express this cross section in terms of $F_2^{D(4)}$ and $R^{D(4)}$ because the data available are predominantly at low $y$ so that there is little sensitivity to $R^{D(4)}$. At fixed $x_{I\!P}$ and $t$ for the range of $y$ of the results presented here ($y \leq 0.428$), $F_2^{D(4)}$ increases by no more than 17% for $0 < R^{D(4)} < \infty$.

The measurement presented here uses data in which the final state colourless remnant is not detected. Therefore no accurate determination of $t$ is possible and the measured cross section amounts to $\frac{\mathrm{d}^3\sigma(ep\rightarrow epX)}{\mathrm{d}x\mathrm{d}Q^2\mathrm{d}x_{I\!P}}$, from which it is possible to determine only $F_2^{D(3)}(x, Q^2, x_{I\!P}) = \int F_2^{D(4)}(x, Q^2, x_{I\!P}, t)\,\mathrm{d}t$ provided that a particular choice is made for $R^{D(4)}$ and its $t$ dependence. The integration is over the range $|\,t_{min}\,| < |\,t\,| < |\,t\,|_{lim}$ where $t_{min}$ is a function of $Q^2$, $W^2$, $M_X^2$ and the mass of the colourless remnant, and $|\,t\,|_{lim}$ is specified by the requirement that all particles in the colourless remnant remain undetected (see section 3). For this measurement, $R^{D(4)}$ is set to 0 for all $t$ and $F_2^{D(3)}$ is evaluated from

$$\frac{\mathrm{d}^3\sigma_{ep\rightarrow epX}}{\mathrm{d}x\mathrm{d}Q^2\mathrm{d}x_{I\!P}} = \frac{4\pi\alpha^2}{xQ^4}\left\{1 - y + \frac{y^2}{2}\right\} F_2^{D(3)}(x, Q^2, x_{I\!P}) \tag{6}$$

following the original procedure of [7, 8].

The above definition of $F_2^{D(3)}(x, Q^2, x_{I\!P})$ renders quantitative comparison with the structure function $F_2(x, Q^2)$ of the proton straightforward [6].

## 2 H1 Apparatus and Kinematic Reconstruction

The data were taken with the H1 detector at the HERA $ep$ collider at DESY in 1993, in which 26.7 GeV electrons were in head–on collision with 820 GeV protons, $\sqrt{s} = 296$ GeV. The H1 detector is described in more detail in [2, 9, 10, 11]. Here the most important aspects necessary to explain the procedures for the analysis are summarised.

In the following, a coordinate system is used with origin at the interaction point and $z$ axis along the proton beam, or forward, direction. The pseudo–rapidity of a final state particle with polar angle $\theta$ in the laboratory is then $\eta = -\ln\tan\frac{\theta}{2}$.

Scattered electrons are measured in the backward electromagnetic calorimeter (BEMC, electromagnetic energy resolution $\sigma_E/E \sim 10\%/\sqrt{E\,(\mathrm{GeV})}$ and overall scale known to within 1.7%) and in a multi–wire proportional chamber (BPC).

Charged particles are detected in central and forward tracking detectors (CTD and FTD). They consist of drift chambers interspersed with multi–wire proportional chambers for fast signals for triggers using charged particles originating from the $z$ range of the event vertex.

Hadronic energy flow in the event final state is measured in the liquid argon (LAr) calorimeter ($-1.51 < \eta < 3.65$). The hadronic energy resolution is $\sigma_E/E \sim 50\%/\sqrt{E\,(\mathrm{GeV})} \oplus 2\%$ (measured in a test beam [12]) and the overall scale is known to within 6%.

The selection of events in which there is no energy flow adjacent to the direction of any proton remnant requires detectors with the best possible coverage in the forward region. The forward "plug" calorimeter (PLUG; $3.54 < \eta < 5.08$) is used in this analysis to "tag" the production of energy above a threshold of 1 GeV. The forward muon detector (FMD) is used in this analysis to "tag" the production of hadrons in the forward pseudo–rapidity range $5.0 < \eta < 6.6$ by detecting and reconstructing track segments due to charged particles produced in secondary interactions of these hadrons in the collimators, the beam pipe, and adjunct material [13, 14].

Two electromagnetic calorimeters (LUMI) situated downstream in the electron beam direction measure electrons and photons from the process $ep \to ep\gamma$ for the purpose of luminosity determination. They are also used in this analysis to help quantify photoproduction background.

The kinematic quantities $x$ and $Q^2$ were reconstructed using the "$\Sigma$ method" [15, 6], which ensures acceptable resolution across the entire kinematic range considered. The procedure, which is relatively insensitive to initial state radiative effects, uses information both from the scattered electron reconstructed using the BEMC and the BPC and from the hadronic energy deposition in the LAr calorimeter and BEMC, together with the event vertex. No attempt was made to use energy flow detected in PLUG and FMD for the purposes of reconstructing the kinematic variables of events.

The mass of the hadronic system excluding the colourless remnant, $M_X$, was determined directly from the calorimeter cells in the LAr calorimeter and BEMC and from the event vertex determined using the tracks reconstructed in the CTD and in the FTD. $\beta$ was then determined using $Q^2$ from above and $M_X$ substituted in equation (4). $x_{I\!P}$ then follows using equation (2).

## 3 Data Taking and Event Selection

The data were obtained with a trigger requiring the presence of a localized energy cluster in the BEMC of 4 GeV or more. The selection procedure described in [6] was used to obtain a sample of DIS $ep$ events, which were then constrained to the kinematic ranges $7.5 < Q^2 < 70\,\mathrm{GeV}^2$ and

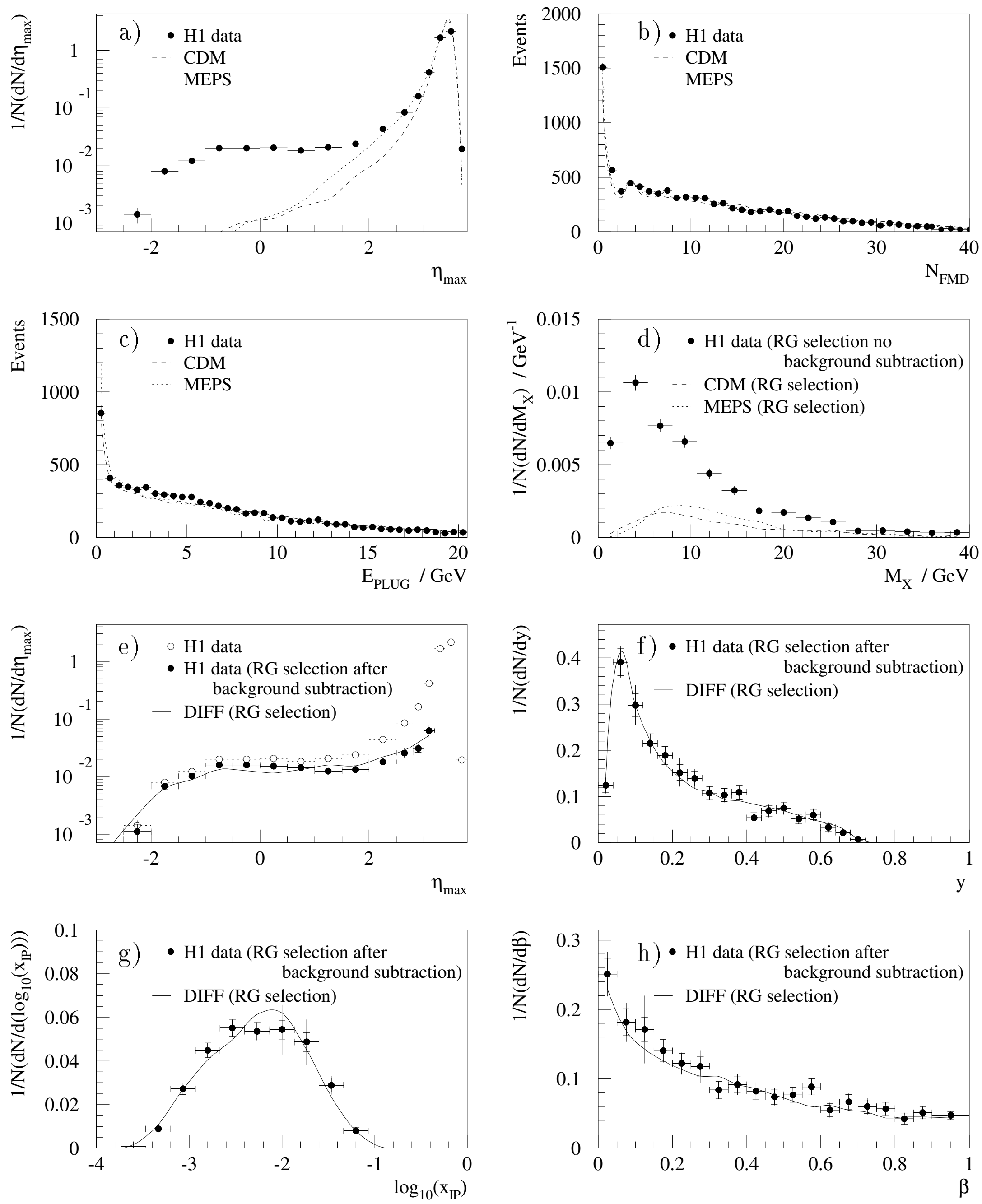


Figure 1: Distributions of a) $\eta_{max}$ measured in the LAr calorimeter for the sample of DIS events; b) the number of charged track segments reconstructed in FMD $N_{\rm FMD}$ per event for DIS events with $\eta_{max} > 3.2$; c) total energy deposition per event in the PLUG for DIS events with $\eta_{max} > 3.2$; d) hadronic invariant mass of the final state system $M_X$ for the selected rapidity gap (RG) events; e) $\eta_{max}$ for DIS events and for the rapidity gap events with the "standard DIS" background subtracted; f) $y$, g) $x_{I\!P}$, and h) $\beta$ for the rapidity gap events with the DIS background subtracted; in a), b), c) and d) the expectations of "standard DIS" simulations (CDM, MEPS), normalised to the data for $\eta_{max} > 3.2$, are also shown and the errors are statistical; in e), f), g) and h) the expectations of the Monte Carlo simulation (DIFF) used to extract the contribution of rapidity gap events in the form of $F_2^{D(3)}$ are also shown, and the systematic error due to due to the DIS background subtraction are included with the statistical error.

$0.03 < y < 0.7$. A total of 16366 events satisfied the selection criteria from an integrated $ep$ luminosity of $271 \pm 14\,\mathrm{nb}^{-1}$.

Figures 1a), b) and c) show spectra which illustrate the response of H1 detectors to these DIS events. Superimposed are two simulated expectations, henceforth referred to as "standard DIS", which are based on a partonic picture and which describe the gross features of DIS data at HERA [6, 16, 17]. They are LEPTO [18] (MEPS), which utilises $O(\alpha_S)$ matrix elements in QCD and parton showers, and a combination of LEPTO and ARIADNE [19] (CDM) in which gluons are radiated from a colour dipole. The parton distribution functions for the proton were taken from MRS(H) [20]. The $(x, Q^2)$ dependence of $F_2(x, Q^2)$ was adjusted to reproduce the most recent measurement of the proton structure function [6].

For the LAr calorimeter (figure 1a), the distribution of $\eta_{max}$, the pseudo–rapidity of the most forward energy cluster [10] with energy greater than 0.4 GeV, is shown. In all following comparisons and analysis, the normalisations of the "standard DIS" simulations are fixed to the number of observed events with $\eta_{max} > 3.2$. Comparison with the "standard DIS" expectations not only demonstrates the excess of events with an interval of pseudo–rapidity adjacent to the proton remnant which is devoid of hadronic energy ($\eta_{max} \lesssim 1.8$), as already reported in [2], but also illustrates how well the LAr calorimeter response and cluster analysis are understood in the forward region ($\eta_{max} \gtrsim 1.8$). In figure 1b) the response of the FMD detector, taken to be the number of track segments reconstructed in a pair of FMD drift chamber layers ($N_{FMD}$), for events with $\eta_{max} > 3.2$, is compared with "standard DIS" expectation. For the PLUG calorimeter (figure 1c), the energy spectrum ($E_{PLUG}$) for these same events is shown, together with "standard DIS" expectation. It can be seen that the measured responses in H1 of FMD ($N_{FMD}$) and of PLUG ($E_{PLUG}$), as well as of the LAr calorimeter ($\eta_{max}$) in the forward region ($\eta \gtrsim 3$), are all very well reproduced by the "standard DIS" simulations for those DIS events with no large rapidity gap.

A sample of events, henceforth referred to as "rapidity gap" events, in which no final state hadronic energy flow is detected adjacent to the proton remnant direction and which is not reproduced by the "standard DIS" simulations, was selected by requiring $E_{PLUG} < 1$ GeV, $N_{FMD} \leq 1$, and $\eta_{max} < 3.2$. These threshold values for $E_{PLUG}$ and $N_{FMD}$ were determined using randomly triggered events in H1, for which the responses of each are then due predominantly to noise coincidences and out of time track segments respectively. In the rapidity gap sample, the remaining background of events which can be described by "standard DIS" simulation was taken to be that due to the CDM simulation because recent measurements of forward energy flow in DIS are known to be well reproduced by it [16]. The uncertainty in this background was estimated using the MEPS simulation, which does not describe well the forward energy flow in DIS. Crucial to this background subtraction are the efficiencies for rejection of events with forward energy flow. They depend on a detailed understanding of the performances of the LAr calorimeter, PLUG, and FMD as "taggers" of forward energy flow. A systematic study of the response of each detector as a function of the presence or absence of signals in the other two and comparison with simulation (CDM and MEPS) yielded a self–consistent set of efficiencies with a quantifiable error [13].

In figure 1d) the distributions in $M_X$ are shown, for the rapidity gap sample, and for the "standard DIS" background (CDM and MEPS). Using Monte Carlo simulation of diffractive DIS events (RAPGAP) [21], the resolution $\sigma(M_X)/M_X$ in $M_X$, determined using LAr and BEMC calorimeter cells, was found to be $\leq 30\%$ for $M_X \geq 6$ GeV and to rise to $\sim 100\%$ as $M_X$ decreased from 6 GeV to threshold (twice the pion mass). The "standard DIS" background remaining after the rapidity gap selection can be seen to vary between 10% and about 50% for $M_X$ less than about 25 GeV. In the following quantitative analysis it is subtracted bin by bin, and a contribution to the systematic uncertainty in the yield of rapidity gap events is taken equal to the difference between the background subtraction calculated using MEPS and that calculated using CDM.

Background, amounting to less than 1% in total, in the rapidity gap sample due to beam gas and beam wall interactions, LAr pile up, cosmic rays, two photon processes and Compton scattering were considered and removed or corrected for as stated in [2]. The level of background due to photoproduction interactions in the rapidity gap sample was determined to be $(5 \pm 5)\%$

in the bin of lowest $x$ and $Q^2$, to be less in other bins, and to be in total 1%, both using Monte Carlo simulation based on the PYTHIA [22] and POMPYT [23] codes, and using those events in the rapidity gap sample in which an electron was detected in the LUMI detectors.

The rapidity gap sample thus selected and used in the analysis in section 4 below, amounted to 1723 events, and 1451 after subtraction of all backgrounds. In figure 1e) the distribution of $\eta_{max}$ is shown both for all DIS events (as in figure 1a) and for the event sample after subtraction of the "standard DIS" background (used to determine $F_2^{D(3)}$ - see below). The errors in the distribution of $\eta_{max}$ in figure 1e) include the systematic uncertainties for the selection based on the forward detectors FMD, PLUG and LAr calorimeter ($\eta_{max} < 3.2$) with the "standard DIS" subtraction.

Below $\eta_{max}$ of 1.8 the distribution of the rapidity gap events in $\eta_{max}$ is everywhere below that for the total DIS sample. This shortfall amounts to 21% in total, of which $(7 \pm 3)\%$ is due to PLUG noise and out of time track segments which fake either or both of energy deposition in the PLUG and more than one reconstructed segment in FMD, and $(5 \pm 3)\%$ is due to "standard DIS" background. The remaining $(9 \pm 4)\%$ is attributed to proton dissociation, secondary particles from which sometimes generate hits in FMD and PLUG. Monte Carlo simulation of DIS diffraction, in which the incident proton dissociates, confirms this interpretation at the observed rate if roughly one third of simulated deep–inelastic diffractive events are assigned as proton dissociation.

The use of a forward rapidity gap to select events in which the proton remnant is colourless also specifies the kinematic range in $t$ of the measurement presented here. In the selected sample of events no particle from the colourless remnant, be it nucleon alone or one of the dissociation products of the proton, may be detected in the detector with the most forward sensitivity, namely FMD ($5.0 < \eta < 6.6$). It follows that $|\, t \,|$ is less than roughly $7\,\mathrm{GeV}^2$ for the range $x < x_{I\!P} < 0.05$ of this measurement.

# 4 Measurement of $F_2^{D(3)}(\beta, Q^2, x_{I\!P})$

The rapidity gap event sample has been used to measure $F_2^{D(3)}(\beta, Q^2, x_{I\!P})$ from the measured cross section by means of equation (6). The results were obtained from the data in the form of $F_2^{D(3)}$ as a function of $\beta$, $Q^2$ and $x$, from which the dependence on $\beta$, $Q^2$ and $x_{I\!P}$ follows using equation (2).

Monte Carlo simulations based on deep inelastic electron–pomeron ($eI\!P$) scattering (RAPGAP) [21] and on diffractive elastic vector meson electroproduction [24, 2] (based on [25, 26]) were used for the determination of acceptance and experimental bias. Both have been demonstrated as necessary to describe well the main features of the data sample [2]. Because the resulting sample is selected on the basis of laboratory pseudo–rapidity $\eta$ in the forward direction, it is confined to small values of $x_{I\!P}$ by virtue of a strong correlation between $\eta_{max}$ and $x_{I\!P}$ [14]. Therefore $F_2^{D(3)}$ is evaluated for the well defined range of the kinematic variable $x_{I\!P} < 0.05$.

$F_2^{D(3)}$ was determined using the measured event numbers in three dimensional bins of $\beta$, $Q^2$ and $x$. The bin acceptances were calculated using Monte Carlo simulation to obtain bin averaged cross sections [13, 14]. The Monte Carlo simulation modelled deep–inelastic $eI\!P$ scattering, in which $I\!P$ structure was taken to be due to a "hard" quark distribution $x_{q/I\!P}(1 - x_{q/I\!P})$ with admixtures of a softer gluon distribution $(1 - x_{g/I\!P})^5$ [21, 7, 8]. The peripheral $t$ dependence for the $I\!P$ flux "in" the proton followed the parameterisation of [27]. Elastic vector meson production was included following [24]. Here $x_{i/I\!P}$, $i = q, g$ are the fractions of the 4–momentum of the $I\!P$ carried by the parton $i$ in the $I\!P$'s structure. When the extracted bin averaged cross sections were included in the Monte Carlo simulation above, the distributions of observables in H1 were described well. Examples are shown as the curves (DIFF) in figures 1e), f), g) and h), where the $e\mathbb{P}$ interaction mix is "hard quark" : "soft gluon" : "elastic VMD" 72 : 21 : 7% in observed events. Note that the quoted proportion of soft gluon events is for the choice of sub–process kinematic cut–off $\hat{p}_T > 0.3\,\mathrm{GeV}$.

The criteria used to choose the kinematic boundaries of each bin included the minimisation of effects due to experimental resolution and smearing for $\beta$ and $x$, and adequate statistics for $Q^2$. No bin with acceptance less than 30% was included. The application of a selection cut $\eta_{max} < 3.2$ for the sample of rapidity gap events ensured that the invariant mass $M_X$, and therefore $\beta$, was well reconstructed. The diffractive Monte Carlo was used to choose bins in $\beta$ for which the average error in $\beta$ never exceeded 65% of the width of the bin, and for which the systematic shifts from true $\beta$ were always $< 5\%$ [13, 14]. None of the bins in $\beta$ included the mass range corresponding to the electroproduction of the vector mesons $\rho(770)$, $\omega(783)$ and $\phi(1020)$. Each bin averaged cross section was then interpolated to a bin centre value in $(\beta, Q^2, x)$ [14], and $F_2^{D(3)}$ was then calculated by straightforward application of equation (6).

Details concerned with the evaluation of all sources of systematic error in the extraction of $F_2^{D(3)}$ are in [13, 14]. They are quoted below as average contributions to $F_2^{D(3)}$ so as to give an indication of their relative significance:

- radiative corrections: 3%;
- uncertainty in acceptance calculation due to absence of higher order QED terms in Monte Carlo simulation: 6%;
- "standard DIS" background subtraction: 17%;
- uncertainties in the diffractive simulation for acceptance correction due to a priori ignorance of physics sub–processes: 11%
- 6% uncertainty in the LAr calorimeter hadronic energy scale: 6%;
- 1.7% uncertainty in the BEMC electromagnetic energy scale: 4%;
- 2 mrad uncertainty in electron scattering angle $\theta_e$: 4%
- uncertainty in experimental acceptance due to a priori ignorance of $F_2^{D(3)}$: 8%.

Having been evaluated for each bin, the above sources of error are combined to form the systematic errors quoted in the results in table 1. To include both proton scattering and proton dissociation, an overall correction was made for the shortfall $(9 \pm 4)\%$ attributed to dissociation (see section 3). Therefore $F_2^{D(3)}$ is evaluated as the total diffractive contribution to the proton structure function $F_2$.

The results for $F_2^{D(3)}$ are shown as the $(\beta, Q^2, x_{\mathbb{P}})$ dependence in figure 2 and as the $(\beta, Q^2, x)$ dependence in table 1. Note that the smallest total error on $F_2^{D(3)}$ is 27%. Therefore there is no sensitivity to any choice of $R^{D(4)}$ in equation (5) and no significant effect due to the assumption $R^{D(4)} = 0$ and the use of equation (6). An overall uncertainty of 8% is not included in the table. It arises from the combination of three uncertainties, in luminosity measurement, in the proportion of proton dissociation in rapidity gap events, and in the selection of rapidity gap events because of PLUG calorimeter noise and random FMD pairs. The results quoted use the "$\Sigma$ method" for kinematic reconstruction. The analysis has also been completed using only the scattered electron to determine the kinematics and the results agree to well within experimental error. Repeating the whole analysis using different cuts, for example no restriction on $\eta_{max}$, produced results for $F_2^{D(3)}$ which did not differ to within systematic error from those quoted.

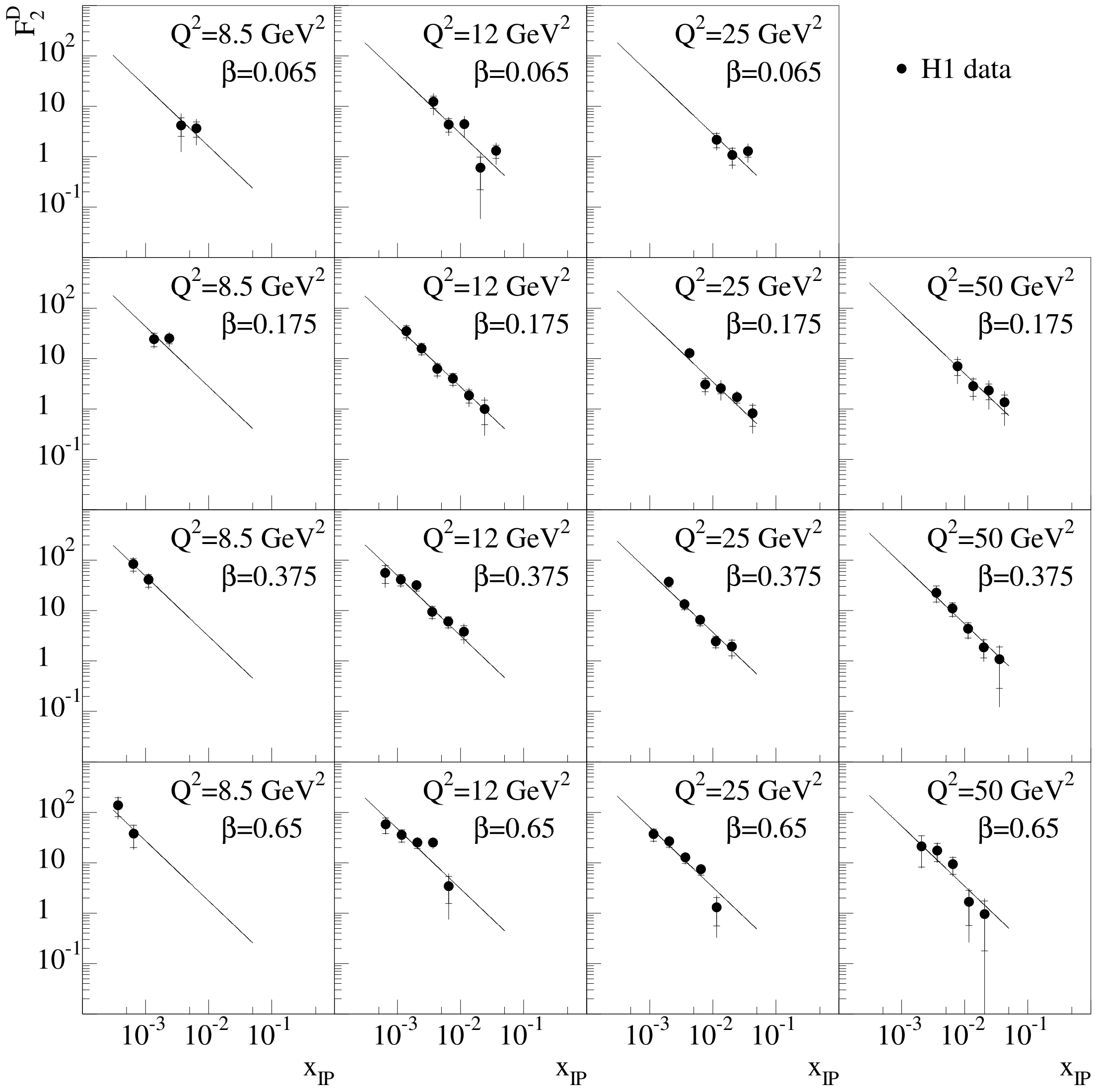


Figure 2: The diffractive contribution $F_2^{D(3)}(\beta, Q^2, x_{I\!P})$ to the proton structure function $F_2$ as a function of $x_{I\!P}$ for different $\beta$ and $Q^2$; the inner error bar is the statistical error; the full error shows the statistical and systematic error added in quadrature; superimposed is the result of the fit establishing a factorisable dependence of the form $\propto x_{I\!P}^{-n}$ (see text). Note that an overall normalisation uncertainty of 8% is not included.

# 5 Factorisation of $F_2^{D(3)}$ and Evidence for Diffraction

Everywhere $F_2^{D(3)}$ is observed to decrease monotonically with increasing $x_{I\!P}$ in the measured range $3 \times 10^{-4} \leq x_{I\!P} < 0.05$. An excellent fit to all data points, irrespective of $\beta$ and $Q^2$, is obtained assuming a polynomial dependence $x_{I\!P}^{-n}$ with a single exponent $n = 1.19 \pm 0.06(stat.) \pm 0.07(syst.)$, $\chi^2/\text{d.f.} = 32.0/46$, 94% C.L. ($\chi^2/\text{d.f.} = 64.5/46$, 4% C.L. assuming only statistical errors). The observed universal dependence on $x_{I\!P}$ is thus a feature of the measurements at the level of statistical accuracy. There is no evidence for any systematic trend in the contributions to $\chi^2$ as a function of $\beta$ and $Q^2$. Using only the reconstructed electron to determine $x$ and $Q^2$ an otherwise identical analysis yielded $n = 1.30 \pm 0.08(stat.) \pm 0.16(syst.)$.

Such a universal dependence on $x_{I\!P}$, independent of $\beta$ and $Q^2$, is expected naively if the deep–inelastic process responsible for rapidity gap events involves a (colourless) target $T$ in the incident proton whose characteristics are not dependent on $x_{I\!P}$, and which carries only a small fraction of the proton's momentum. The dependence of $F_2^{D(3)}(\beta, Q^2, x_{I\!P})$ then factorises into the

| $Q^2 = 8.5$ GeV$^2$ | | | | | | |
|---|---|---|---|---|---|---|
| $\beta$ | $x$ | $F_2^{D(3)}$ | ST | SY | AC | FB |
| 0.065 | .00024 | 4.21 | 1.68 | 2.44 | 0.58 | 0.16 |
| 0.065 | .00042 | 3.65 | 1.23 | 1.51 | 0.77 | 0.23 |
| 0.175 | .00024 | 24.40 | 7.33 | 4.50 | 0.54 | 0.04 |
| 0.175 | .00042 | 25.14 | 5.62 | 6.38 | 0.70 | 0.02 |
| 0.375 | .00024 | 84.85 | 23.75 | 17.53 | 0.48 | 0.01 |
| 0.375 | .00042 | 40.85 | 11.48 | 8.97 | 0.79 | 0.08 |
| 0.650 | .00024 | 139.25 | 56.85 | 35.43 | 0.35 | 0.00 |
| 0.650 | .00042 | 37.66 | 17.77 | 8.12 | 0.76 | 0.05 |

| $Q^2 = 12.0$ GeV$^2$ | | | | | | |
|---|---|---|---|---|---|---|
| $\beta$ | $x$ | $F_2^{D(3)}$ | ST | SY | AC | FB |
| 0.065 | .00024 | 12.45 | 3.39 | 4.72 | 0.52 | 0.08 |
| 0.065 | .00042 | 4.38 | 1.29 | 1.22 | 0.58 | 0.24 |
| 0.065 | .00075 | 4.43 | 0.87 | 1.84 | 0.57 | 0.16 |
| 0.065 | .00133 | 0.60 | 0.38 | 0.39 | 0.55 | 0.68 |
| 0.065 | .00237 | 1.31 | 0.38 | 0.47 | 0.30 | 0.29 |
| 0.175 | .00024 | 34.99 | 9.60 | 8.40 | 0.62 | 0.06 |
| 0.175 | .00042 | 15.82 | 3.94 | 2.67 | 0.65 | 0.08 |
| 0.175 | .00075 | 6.20 | 1.72 | 1.38 | 0.69 | 0.12 |
| 0.175 | .00133 | 3.99 | 1.05 | 0.77 | 0.73 | 0.26 |
| 0.175 | .00237 | 1.85 | 0.54 | 0.52 | 0.84 | 0.37 |
| 0.175 | .00421 | 1.00 | 0.51 | 0.49 | 0.48 | 0.43 |
| 0.375 | .00024 | 56.41 | 21.72 | 17.15 | 0.53 | 0.02 |
| 0.375 | .00042 | 41.30 | 10.18 | 8.15 | 0.67 | 0.02 |
| 0.375 | .00075 | 31.88 | 7.58 | 4.65 | 0.46 | 0.01 |
| 0.375 | .00133 | 9.54 | 2.64 | 1.70 | 0.65 | 0.12 |
| 0.375 | .00237 | 6.05 | 1.53 | 0.89 | 0.73 | 0.18 |
| 0.375 | .00421 | 3.84 | 1.18 | 1.17 | 0.66 | 0.19 |
| 0.650 | .00042 | 58.00 | 19.94 | 8.08 | 0.63 | 0.03 |
| 0.650 | .00075 | 35.34 | 9.71 | 4.78 | 0.79 | 0.03 |
| 0.650 | .00133 | 25.27 | 6.03 | 3.44 | 0.77 | 0.04 |
| 0.650 | .00237 | 25.04 | 4.70 | 3.95 | 0.70 | 0.03 |
| 0.650 | .00421 | 3.44 | 1.88 | 1.93 | 0.71 | 0.31 |

| $Q^2 = 25.0$ GeV$^2$ | | | | | | |
|---|---|---|---|---|---|---|
| $\beta$ | $x$ | $F_2^{D(3)}$ | ST | SY | AC | FB |
| 0.065 | .00075 | 2.20 | 0.70 | 0.51 | 0.63 | 0.40 |
| 0.065 | .00133 | 1.08 | 0.39 | 0.32 | 0.53 | 0.48 |
| 0.065 | .00237 | 1.29 | 0.30 | 0.43 | 0.37 | 0.20 |
| 0.175 | .00075 | 12.89 | 2.42 | 2.53 | 0.68 | 0.06 |
| 0.175 | .00133 | 3.08 | 0.90 | 0.85 | 0.76 | 0.30 |
| 0.175 | .00237 | 2.57 | 0.57 | 0.95 | 0.80 | 0.27 |
| 0.175 | .00421 | 1.71 | 0.40 | 0.41 | 0.60 | 0.31 |
| 0.175 | .00750 | 0.82 | 0.37 | 0.33 | 0.34 | 0.39 |
| 0.375 | .00075 | 37.64 | 7.85 | 6.30 | 0.51 | 0.02 |
| 0.375 | .00133 | 13.52 | 3.09 | 1.94 | 0.64 | 0.11 |
| 0.375 | .00237 | 6.54 | 1.52 | 0.90 | 0.71 | 0.17 |
| 0.375 | .00421 | 2.46 | 0.64 | 0.40 | 0.91 | 0.27 |
| 0.375 | .00750 | 1.93 | 0.65 | 0.55 | 0.73 | 0.35 |
| 0.650 | .00075 | 37.02 | 10.13 | 6.01 | 0.77 | 0.02 |
| 0.650 | .00133 | 26.54 | 6.31 | 3.99 | 0.70 | 0.04 |
| 0.650 | .00237 | 12.76 | 2.95 | 1.87 | 0.82 | 0.06 |
| 0.650 | .00421 | 7.43 | 1.71 | 0.99 | 0.81 | 0.11 |
| 0.650 | .00750 | 1.30 | 0.74 | 0.63 | 0.92 | 0.34 |

| $Q^2 = 50.0$ GeV$^2$ | | | | | | |
|---|---|---|---|---|---|---|
| $\beta$ | $x$ | $F_2^{D(3)}$ | ST | SY | AC | FB |
| 0.175 | .00133 | 7.04 | 2.44 | 3.12 | 0.70 | 0.09 |
| 0.175 | .00237 | 2.84 | 1.06 | 0.87 | 0.77 | 0.26 |
| 0.175 | .00421 | 2.33 | 0.80 | 1.09 | 0.55 | 0.25 |
| 0.175 | .00750 | 1.35 | 0.55 | 0.71 | 0.33 | 0.18 |
| 0.375 | .00133 | 22.68 | 7.85 | 3.64 | 0.60 | 0.09 |
| 0.375 | .00237 | 11.03 | 3.32 | 1.83 | 0.71 | 0.11 |
| 0.375 | .00421 | 4.34 | 1.45 | 0.80 | 0.82 | 0.20 |
| 0.375 | .00750 | 1.89 | 0.74 | 0.54 | 0.85 | 0.32 |
| 0.375 | .01330 | 1.09 | 0.81 | 0.54 | 0.39 | 0.55 |
| 0.650 | .00133 | 21.33 | 13.07 | 3.75 | 0.50 | 0.06 |
| 0.650 | .00237 | 17.47 | 6.95 | 2.95 | 0.61 | 0.05 |
| 0.650 | .00421 | 9.34 | 3.45 | 2.07 | 0.70 | 0.10 |
| 0.650 | .00750 | 1.69 | 1.13 | 0.89 | 0.92 | 0.39 |
| 0.650 | .01330 | 0.96 | 0.78 | 0.62 | 0.83 | 0.50 |

Table 1: The diffractive contribution $F_2^{D(3)}$ to the proton structure function $F_2$ as a function of $\beta$, $Q^2$ and $x$; ST is the statistical error, SY is the total systematic error, AC is the (smeared) acceptance, and FB the proportion of the signal calculated to be background (see text). Not included in the errors is an overall normalisation uncertainty of 8%.

product of a universal term ($f_{T/p}(x_{I\!P}) \propto x_{I\!P}^{-n}$), which describes the "flux" of $T$ "in" the proton, and a term which describes any structure of $T$ and which is a function of only $\beta$ and $Q^2$. The electron scattering cross section for the process $ep \rightarrow eXp, N^*$ etc. can then be written

$$\frac{\mathrm{d}^3\sigma_{ep\rightarrow epX}}{\mathrm{d}\beta \mathrm{d}Q^2 dx_{I\!P}} = \frac{\mathrm{d}^2\sigma_{eT\rightarrow eX}}{\mathrm{d}\beta\mathrm{d}Q^2} \cdot f_{T/p}(x_{I\!P}) \tag{7}$$

where $\frac{\mathrm{d}^2\sigma_{eT\rightarrow eX}}{\mathrm{d}\beta\mathrm{d}Q^2}$ describes the deep–inelastic scattering of the electron off $T$.

If the colourless component $T$ of the proton is taken to be well parameterised as a "Reggeised" hadronic exchange, then the $x_{I\!P}$ dependence of the flux factor is specified by the leading Regge trajectory $\alpha(t)$ in the "asymptotic limit" $x_{I\!P} \rightarrow 0$, $t/s \rightarrow 0$. The dependence takes the form $x_{I\!P}^{-[2\alpha(t)-1]}$ [28, 29, 30]. In this measurement we perforce integrate over $t$. To good approximation, $\alpha(t)$ may be replaced by $\alpha_{t=0}$ because the $t$ distribution of the soft hadronic proton interaction is likely to be "peripheral" and the $t$ dependence of $\alpha(t)$ is likely to be slight.

The observed $x_{I\!P}$ dependence corresponds to $\alpha_{t=0} = 1.10 \pm 0.03(stat.) \pm 0.04(syst.)$. It is therefore consistent with the leading (effective) trajectory which describes phenomenologically "soft hadronic" diffractive interactions, namely the $I\!P$ with $\alpha(t) = \alpha_{t=0} + \alpha' t$ and $\alpha_{t=0} = 1.085$, $\alpha' = 0.25\,\mathrm{GeV}^{-2}$ [31, 32]. If the $t$ distribution of proton diffraction is here like that in soft $pp$ collisions, namely peripheral with a dependence $e^{bt}$ with $b > 1$, then the systematic error, which arises by ignoring any $t$ dependence of $\alpha(t)$ of size given by the slope $\alpha' = 0.25\,\mathrm{GeV}^{-2}$ of the $I\!P$ trajectory, is $< 4\%$. Note that the leading meson Regge trajectories, the $f_2(1270)/\omega(783)$ for a diffractive–like process with no isospin exchange, and the exchange degenerate $\rho(770)/a_2(1320)$ for a process involving isospin exchange, have intercept $\alpha_{t=0} \sim 0.5$, giving rise to an $x_{I\!P}$ dependence which is much less steep. Parameterisations of pion exchange, either "Reggeised" ($\alpha_{t=0} \sim 0$) or otherwise, have only a slight dependence on $x_{I\!P}$. Therefore the interpretation of the rapidity gap events in DIS at low Bjorken–$x$ as being due in the main either to diffractive scattering or to diffractive dissociation of the incident proton can be made without ambiguity.

The $x_{I\!P}$ dependence observed here does not specify the $M_X^2$ dependence in the process $ep \to epX$ without a further assumption for the $\beta$ dependence of $\frac{\mathrm{d}^3\sigma_{ep\to epX}}{\mathrm{d}\beta \mathrm{d}Q^2 \mathrm{d}x_{I\!P}}$. However, note that $x_{I\!P} = M_{eX}^2/s$ where $M_{eX}^2$ is the invariant mass squared recoiling against the proton in the inclusive process $pe \to p(eX)$. Therefore the observation of an $x_{I\!P}$ dependence $\propto x_{I\!P}^{-n}$ in the process $ep \to epX$ is equivalent to a dependence on $M_{eX}^2$ of $(M_{eX}^2)^{-n}$ at fixed $ep$ CM energy $\sqrt{s}$ in the inclusive process $pe \to p(eX)$. It is the distribution in missing invariant mass squared $M_Y^2$ of the form $\propto (M_Y^2)^{-[2\alpha(t)-1]}$, $\alpha_{t=0} = 1.085$, $\alpha' = 0.25\,\mathrm{GeV}^{-2}$ in the soft hadronic interaction $pp \to pY$ which is characteristic of high energy inelastic diffraction and which specifies the effective $I\!P$ trajectory $\alpha(t)$ in $pp$ diffractive dissociation [32].

In calculations which use the BFKL QCD formalism of $I\!P$ dynamics, the $I\!P$ is found to be "hard" with an intercept ($\alpha_{t=0} = 1+\varepsilon$, $\varepsilon \lesssim 0.5$) [33, 34]. Combining in quadrature the statistical and systematic errors of the measurement of the $x_{I\!P}$ dependence above, the intercept cannot exceed 1.25 (i.e. $\varepsilon \leq 0.25$) with 99.7% confidence. This does not rule out such a "hard" $I\!P$ if it contributes together with a soft component, such as that described above. A recent calculation, based on a BFKL approach, suggests also that the simplest factorisation with an $x_{I\!P}$ dependence $\propto x_{I\!P}^{-n}$ may not strictly hold [35]. The accuracy of this measurement of the $x_{I\!P}$ dependence does not exclude such a possibility.

# 6 The Deep–Inelastic Structure of the Pomeron

The observation that rapidity gap events in DIS are dominantly of a diffractive nature, and the evidence for a simple factorisation of the structure function $F_2^{D(3)}(\beta, Q^2, x_{I\!P})$ over values of $x_{I\!P}$ in the range $3 \times 10^{-4} < x_{I\!P} < 0.05$ for different values of $\beta$ and $Q^2$, lead naturally to the interpretation of the $\beta$ and $Q^2$ dependence of $F_2^{D(3)}$ as a measure of the deep–inelastic structure of diffractive exchange. If such exchange is taken phenomenologically to be described by an effective Regge trajectory, this interpretation amounts to the deep–inelastic structure of the $I\!P$.

In figure 3 are shown the $\beta$ and $Q^2$ dependences of the integral

$$\tilde{F}_2^D(\beta, Q^2) = \int_{x_{I\!P_L}}^{x_{I\!P_H}} F_2^{D(3)}(\beta, Q^2, x_{I\!P})\,\mathrm{d}x_{I\!P}, \tag{8}$$

which, assuming factorisation, is proportional to the structure function of the $I\!P$. The range of integration, $x_{I\!P_L} = 3 \times 10^{-4}$ and $x_{I\!P_H} = 0.05$ is chosen to span the entire $x_{I\!P}$ range of measurements of $F_2^{D(3)}$. $\tilde{F}_2^D$ is evaluated assuming that the factorisation hypothesis with the measured dependence on $x_{I\!P}$ is a good description over this range of integration. The assumption is therefore made that, for certain values of $\beta$ and $Q^2$, the observed $x_{I\!P}$ dependence is valid beyond the measured range in $x_{I\!P}$, including values which are kinematically inaccessible in this measurement. Note therefore that, unlike $F_2^{D(3)}$ or any integration of it over kinematically accessible values of $\beta$, $Q^2$ and $x_{I\!P}$, $\tilde{F}_2^D$ is not a measure of the diffractive contribution to $F_2$. The errors in the results for $\tilde{F}_2^D(\beta, Q^2)$ include the contributions from the uncertainty above (both statistical and systematic) in the "flux" dependence on $x_{I\!P}$. It is convenient to define $\tilde{F}_2^D(\beta, Q^2)$ in this way to avoid the need to specify the normalisation of the unknown diffractive, or $I\!P$, "flux" in the proton when presenting the data in a form which is suitable for direct comparison with theoretical expectation for $I\!P$ structure.

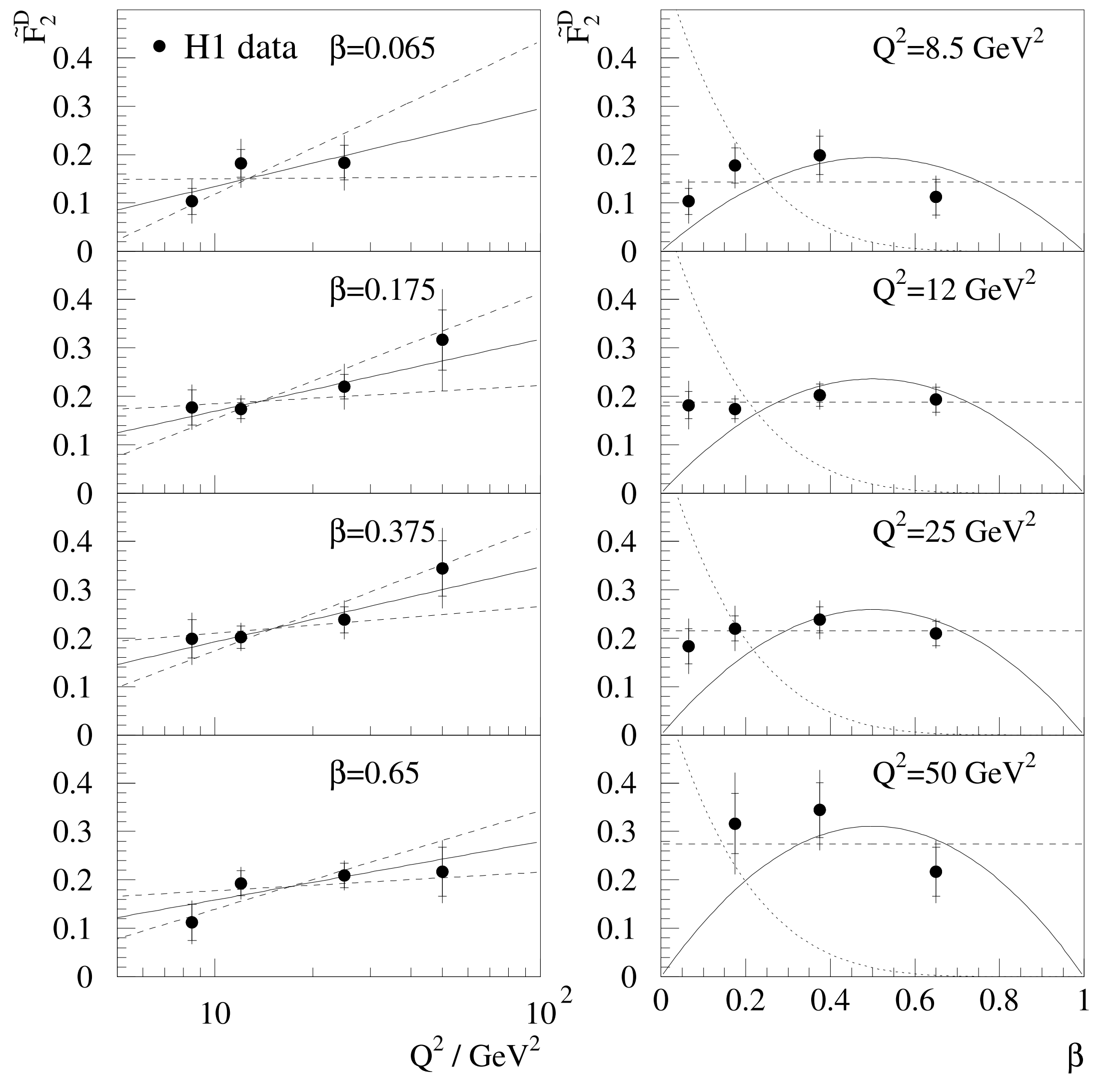


Figure 3: Dependence of $\tilde{F}_2^D(\beta, Q^2)$ on $Q^2$ and $\beta$; superimposed on the $Q^2$ dependence are the results of fits at each $\beta$ which assume leading logarithmic scaling violations; the best fit (continuous curve) and the curves corresponding to a change of $\pm 1$ standard deviation (dashed curves) in the slope are shown; superimposed on the $\beta$ dependence are the simplest $q\bar{q}$ expectation for $I\!P$ structure - $[\beta(1-\beta)]$ (continuous curve), and a constant dependence (dashed curve), for which the overall normalisations are determined from fits to the data; also displayed is a dependence of the form $[(1-\beta)^5]$ (dotted curve) with arbitrary normalisation. Note that an overall normalisation uncertainty of 8% is not included.

There is no evidence for any substantial $Q^2$ dependence of $\tilde{F}_2^D$. Deep (high $Q^2$) diffractive interactions are thus broadly of a scale invariant, and therefore point-like, nature. Furthermore, $\tilde{F}_2^D$ is observed to have little dependence on $\beta$ with contributions throughout the measured range ($0.065 < \beta < 0.65$). Therefore the structure which is resolved by the electron in the high $Q^2$ diffractive interaction carries only a fraction of the $I\!P$'s momentum, implying that the $I\!P$ has its own sub–structure which may presumably be attributed to point-like partons.

A fit to the hypothesis of a linear $\log_{10} Q^2$ dependence demonstrates that the data are consistent with zero slope to within $\sim 1$ standard deviation ($\sigma$). The errors on the slopes in the fits shown in figure 3 amount to $\sigma = 0.09\,(\log_{10}\,\mathrm{GeV}^2)^{-1}$ for all $\beta$ except that at $\beta = 0.065$ for which $\sigma = 0.15\,(\log_{10}\,\mathrm{GeV}^2)^{-1}$. Therefore the accuracy of this first measurement of the $Q^2$ dependence of $\tilde{F}_2^D$ is such that the possibility of "scaling violations", symptomatic of QCD, may be admitted. Furthermore, either they may be $\beta$ dependent and thus characteristic of that observed for the structure function of a hadron such as the proton, or they may be insensitive to $\beta$ and thus characteristic of the structure function of a "dressed" point–like field quantum such as the photon.

Also shown in figure 3 superimposed on the $\beta$ dependence of $\tilde{F}_2^D$ is the expectation based on the simplest $q\bar{q}$ picture of deep–inelastic diffraction, namely a "hard" quark $\beta(1-\beta)$ dependence [7, 8]. Such a dependence has been justified in an approach in which $q$, $\bar{q}$ or both "scatter" diffractively off the proton [32, 35]. In such a picture, diffractive quark scattering at high energy amounts to the exchange of two or more gluons and has a leading order energy dependence of Regge form [36]. There is a suggestion that the observed $\beta$ dependence may exceed this simple $q\bar{q}$ expectation as $\beta \rightarrow 0$, which is naturally to be expected in any quantum chromodynamic interpretation which includes gluons as well as quarks. A fit assuming no dependence of $\tilde{F}_2^D$ on $\beta$ is equally acceptable. The ansatz of a soft dependence $(1-\beta)^5$ is completely ruled out. The lack of measurements at large $\beta$, where elastic vector meson production contributes, means that no conclusion can be drawn concerning the existence or otherwise of a "super–hard" component in $I\!P$ structure, first suggested by Brandt et al. [37].

The dependence of $\tilde{F}_2^D$ on $Q^2$ and on $\beta$, the appropriate Bjorken–$x$ like variable, resembles well established measurements of the structure functions $F_2$ of hadrons in that it is consistent with an understanding based on asymptotically free partons. It however contrasts with them in that the Bjorken–$x$ dependences of the structure functions $F_2$ of hadrons are all observed to decrease substantially with increasing Bjorken–$x$. This suggests the simplest possible interpretation for the sub–structure of the $I\!P$, namely that due to two "valence–like" partons which share the majority of the 4–momentum of the $I\!P$, together with modifications at low $\beta$ due to QCD evolution.

# 7 Summary and Conclusions

The contribution to inclusive deep–inelastic electron–proton scattering (DIS) of events, in which a region of pseudo–rapidity adjacent to the proton remnant direction is devoid of hadronic energy and which is not described in the framework of our present partonic understanding of DIS, has been evaluated in the form of a "diffractive structure function" $F_2^{D(3)}(\beta, Q^2, x_{I\!P})$.

The dependence of $F_2^{D(3)}$ on $x_{I\!P}$, which may be interpreted as the fraction ($x_{I\!P/p}$) of the 4–momentum carried by the colourless component of the proton with which the electron interacts, is measured to be $x_{I\!P}^{-n}$ with $n = 1.19 \pm 0.06(stat.) \pm 0.07(syst.)$. This dependence is found to be universal, irrespective of the deep–inelastic scattering variables $\beta$ and $Q^2$. This is as expected if the electron–proton cross section can be factorised into the product of a term which describes the "flux" of colourless component of the proton and a term which corresponds to the cross section for the interaction of the latter with the electron.

In the framework of "Reggeised" hadronic exchange in the $t$–channel which couples to the incident proton, the dependence of $F_2^{D(3)}$ on $x_{I\!P}$ may be interpreted as the intercept $\alpha_{t=0} = 1.10 \pm 0.03(stat.) \pm 0.04(syst.)$ of the leading Regge trajectory. The latter is consistent with that of the pomeron trajectory which describes phenomenologically the energy dependence of soft hadronic diffraction, and is inconsistent with the intercepts $\alpha_{t=0} \sim 0.5$ of the leading meson Regge trajectories. The origin of "rapidity gap events" in deep–inelastic lepton nucleon scattering is therefore demonstrated unambiguously to be predominantly diffractive, and the colourless component of the proton to be consistent with the pomeron. The precision of the measurement of $\alpha_{t=0}$ does not exclude the possibility of a contribution to deep–inelastic diffractive scattering from a harder BFKL motivated pomeron trajectory with a higher intercept.

The deep–inelastic structure of the pomeron is observed to be consistent with scale invariance for all measured values of the appropriate "Bjorken–$x$" like variable $\beta$. $F_2^{D(3)}$ is observed to be non–zero for a significant range of values of $\beta$, demonstrating a substantial inelastic contribution.

The sub-structure which is resolved in diffractive deep–inelastic electron scattering thus carries only a fraction of the momentum of the pomeron, meaning, when taken together with the observation of broad consistency with scale invariance, that this sub–structure may presumably be attributed to point-like partons.

## Acknowledgments

We are grateful to the HERA machine group whose outstanding efforts have made and continue to make this experiment possible. We thank the engineers and technicians for their work in constructing and now maintaining the H1 detector, our funding agencies for financial support, the DESY technical staff for continual assistance, and the DESY directorate for the hospitality which they extend to the non–DESY members of the collaboration. We also acknowledge much help with the theoretical interpretation of our results from many colleagues, in particular G. Ingelman.

## References

[1] M. Derrick et al. (ZEUS Collaboration) Phys. Lett. **B315** (1993) 481.

[2] T. Ahmed et al. (H1 Collaboration), Nucl. Phys. **B429** (1994) 477.

[3] F. E. Low, Phys. Rev. **D12** (1975) 163.

[4] S. Nussinov, Phys. Rev. Lett. **34** (1975) 1286, Phys. Rev. **D14** (1976) 246.

[5] G. Ingelman and P. Schlein, Phys. Lett. **B152** (1985) 256,
R. Bonino et. al. (UA8 Collaboration), Phys. Lett. **B211** 239 (1988).

[6] T. Ahmed et al. (H1 Collaboration), "A Measurement of the Proton Structure Function $F_2(x, Q^2)$", DESY preprint DESY 95–006 (1995), to appear in Nucl. Phys. **B**.

[7] G. Ingelman and K. Janson–Prytz, "The Pomeron Structure Function and QCD at Small–$x$", in Proceedings of the Workshop "Physics at HERA", p. 233, October 1991, ed. W. Buchmüller and G. Ingelman.

[8] G. Ingelman and K. Prytz, Zeit. Phys. **C58** (1993) 285.

[9] I. Abt et al. (H1 Collaboration), "The H1 Detector at HERA", DESY preprint DESY 93–103 (1993).

[10] B. Andrieu et al. (The H1 Calorimeter Group), Nucl. Inst. Meth. **A336** (1993) 460.

[11] H. I. Cronström et al. Nucl. Inst. Meth. **A340** (1994) 304.

[12] B. Andrieu et al. (The H1 Calorimeter Group), Nucl. Inst. Meth. **A336** (1993) 499.

[13] A. Mehta, "Measurement of the Diffractive Proton Structure Function and Calibration of the Forward Muon Detector at H1", PhD thesis (University of Manchester), 1994 (unpublished).

[14] J. Phillips, "The Deep–Inelastic Structure of Diffraction", PhD thesis (University of Manchester), 1995 (unpublished).

[15] U. Bassler and G. Bernardi, "On the Kinematic Reconstruction of Deep Inelastic Scattering at HERA: the Sigma Method", DESY 94–231 (1994), submitted to Nucl. Instr. and Meth.

[16] I. Abt et al. (H1 Collaboration), Zeit. Phys. **C63** (1994) 377.

[17] I. Abt et al. (H1 Collaboration), Zeit. Phys. **C61** (1994) 59.

[18] G. Ingelman, "LEPTO 6.1", unpublished program manual, and in Proc. of the Workshop "Physics at HERA", 1366, ed. W. Buchmüller and G. Ingelman, Hamburg (1991)
H. Bengtsson, G. Ingelman and T. Sjöstrand, Nucl. Phys. **B301** (1988) 554.

[19] L. Lönnblad, Comput. Phys. Commun. **71** (1992) 15.

[20] A. D. Martin, W. J. Stirling and R. G. Roberts, Phys. Rev. **D50** (1994) 6734.

[21] H. Jung, "Hard Diffractive Scattering in High Energy $ep$ Collisions and the Monte Carlo Generator RAPGAP", DESY preprint DESY 93–182 (1993), to appear in Comput. Phys. Commun.

[22] H.–U. Bengtsson and T. Sjöstrand, Comput. Phys. Commun. **46** (1987) 43.

[23] P. Bruni and G. Ingelman, "POMPYT", in Proc. of the Europhysics Conference, Marseilles, France, July 1993, ed. J. Carr and M. Perrottet, p.595, and unpublished program manual.

[24] B. List, "Diffraktive $J/\psi-$Produktion in Elektron–Proton–Stößen am Speicherring HERA", Diploma Thesis (Tech. Univ. Berlin), 1993 (unpublished).

[25] J. J. Sakurai, Phys. Rev. Lett. **22** (1969) 981
J. J. Sakurai and D. Schildknecht, Phys. Lett. **40B** (1972) 121.

[26] T. H. Bauer, R. D. Spital, D. R. Yennie, F. M. Pipkin, Rev. Mod. Phys. **50** (1978) 261.

[27] E. L. Berger et al. Nucl. Phys. **B286** (1987) 704
K. H. Streng, in Proc. of the Workshop "Physics at HERA", p. 365, ed. R. D. Peccei, Hamburg (1987); CERN preprint CERN–TH 4949 (1988).

[28] T. Regge, Nuov. Cim. **14** (1959) 951, Nuov. Cim. **18** (1960) 947.

[29] G. Chew, S. Frautschi, S. Mandelstam, Phys. Rev. **126** (1962) 1202.

[30] P. Collins and E. Squires, "An Introduction to Regge Theory and High Energy Physics", Cambridge University Press, Cambridge (1977).

[31] S. Belforte (CDF Collaboration), "Measurement of the Elastic, Total, and Diffraction Cross Sections at Tevatron energies", in Proc. of the Europhysics Conference, Marseilles, France, July 1993, ed. J. Carr and M. Perrottet, p.578, July 1993, and Fermilab preprint Fermilab–Conf–93/358–E (1993).

[32] A. Donnachie and P. Landshoff, Nucl. Phys. **B303** (1988) 634.

[33] L. N. Lipatov, Sov. Phys. JETP **63** (1986) 904.

[34] É. A. Kuraev, L. N. Lipatov, and V. S. Fadin, Sov. Phys. JETP **45** (1977) 199
Ya. Ya. Balitskiǐ and L. N. Lipatov, Sov. J. Nucl. Phys. **28** (1978) 822.

[35] M. Genovese, N. N. Nikolaev, B. G. Zakharov, "Diffractive DIS from the generalised BFKL pomeron. Predictions for HERA.", Institut für Kernphysik, KFA, Jülich preprint KFA–IKP(Th)–1994–37.

[36] P. V. Landshoff and O. Nachtmann, Zeit. Phys. **C35** (1987) 405.

[37] A. Brandt et al. (UA8 Collaboration), Phys. Lett. **B297** (1992) 417.